Dry and hydraulic extensile fracturing of porous impermeable materials

J.H.M. Visser and J.G.M. van Mier
Delft University of Technology, Faculty of Civil Engineering

Extensile hydraulic fracturing of mortar is investigated and compared to extensile dry fracturing of sandstone. The extensile fracture experiments have been performed in a Hookean cell in deformation control. The cell allows for axial loading and radial fluid pressure loading of cylindrical specimens. Variables in the experiments are the load path and the degree of saturation. In the dry fracturing tests, the sandstone specimens are sleeved. In the hydraulic fracture experiments, the mortar specimens are not sleeved so that the radial fluid pressure is free to enter the notch and the fracture once it is initiated. In the dry fracturing experiments, the sandstone becomes more ductile for increasing hydrostatic stress. In the hydraulic fracture experiments, the mortar remains brittle. The results of the hydraulic fracture experiments are very similar for the unsaturated mortar (degree of saturation 69%) and the saturated mortar (degree of saturation 100%). The saturated mortar behaves stiffer and has higher failure stresses due to the effect of pore pressures. Fracture propagation in the saturated mortar requires lower stresses, although the difference with fracture propagation in the unsaturated mortar is minor.

Key words: **extensile dry fracturing experiments, extensile hydraulic fracturing experiments, load path, degree of saturation, sandstone, mortar, pore pressure**

1 Introduction

Fracturing of engineering materials is extensively investigated for many years (e.g. Van Mier, 1997). The importance of this research is evident since failure or collapse of structures may have serious consequence of economic and human nature. Fracturing of structures occurs when mechanical loads exceed the strength of the material of the structures. A special case is the fracturing of material in a water environment, such as for instance for dams and jack-up platforms (Twort et al., 1994, Clauss et al., 1992, Brühwiler and Saouma, 1990). The structures are then not only loaded by the water pressure on the material but also inside pre-existing surface cracks, by the open communication of the cracks and the water environment. The fluid pressure in the fracture wedges the fracture further open. The pressure driven fractures are called hydraulic fractures, as contrary to dry fractures in which no pressure load in the fracture exists (see Fig. 1). Neglecting the fluid pressure in the fracture will give rise to seriously underestimation of, for instance, stability of structures (Saouma et al., 1989). Only recently, research on fluid driven fractures in civil engineering structures have attained some attention (Bourdarot et al., 1994).

HERON, Vol. 41, No. 4 (1996) ISSN 0046-7316

One of the main factors influencing the contribution of the fracture pressure to the fracture propagation is the degree of water saturation of porous materials (Alonso et al., 1987, Schmitt and Zoback, 1992). Since hydraulic fracturing occurs in a water environment (or some other fluid environment), the porous materials are often fully saturated by penetration of the water. Mechanical loading gives rise to pore fluid pressures which act as closing pressures on the fracture (Fig. 1c). Pore water is thus expected to reduce the effect of the fracture pressure (Thiercelin et al., 1987).

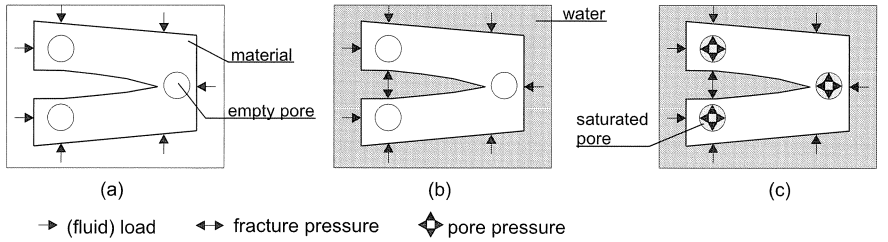

Fig. 1. Definition of fractures: dry fracture (a), hydraulic fracture in a dry material (b) and hydraulic fracture in a saturated material (c).

The aim of this paper is to investigate extensile hydraulic fracturing of impermeable mortar. Variables in the experiments are the load path and the degree of saturation. The hydraulic fracturing experiments are compared to dry fracturing experiments. The dry fracturing experiments, however, are performed on sandstone. The experimental set-up and test performance are described in Section 2. In Section 3, a description of the sandstone and mortar is given. The influence of the degree of saturation on the materials is discussed in Section 4. The dry fracturing experiments are given in Section 5, while the hydraulic fracturing experiments are presented in Section 6. Conclusions are given in Section 7.

The stress convention in this paper is negative for tension and positive for compression. The peak stress of a response curve is called failure stress. The uniaxial tensile failure stress is assumed to be equal to the tensile strength, and the uniaxial compressive failure stress is assumed to be equal to the compressive strength of the materials.

2 Experiments

The experiments are performed on cylindrical specimens in a Hookean cell (Fig. 2). All specimens have the same dimensions (300 × ϕ 100 mm) and contain a circular notch (depth/width 5 × 5 mm). The specimens can be loaded independently by a radial fluid pressure and an (tensile or compressive) axial load. The specimens can move freely in the longitudinal direction. A detailed discussion of the experimental set-up, boundary conditions and test performance is given in Visser and Van Mier, 1994.

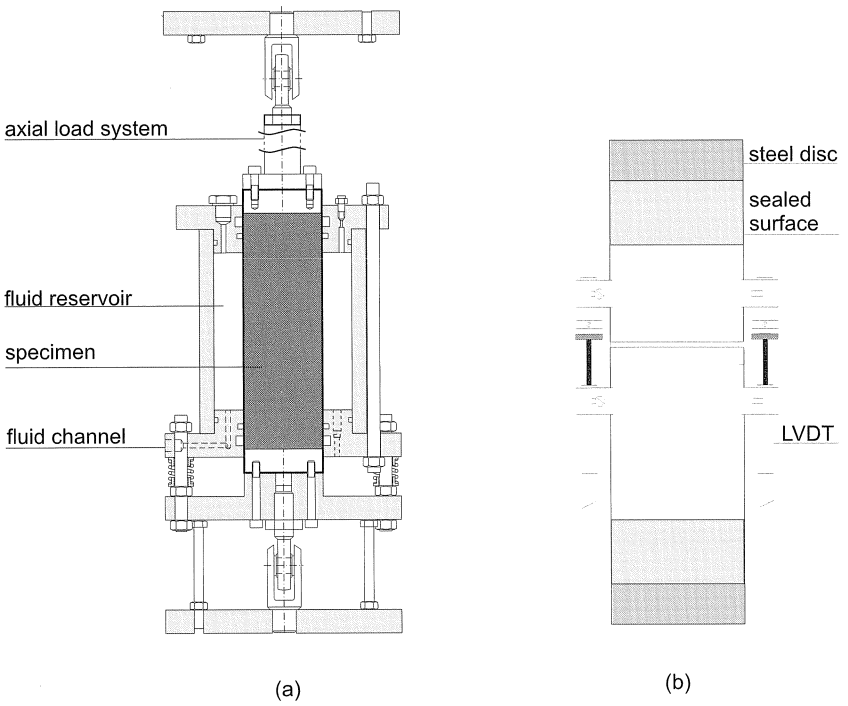

Fig. 2. Hookean cell (a) and instrumented specimen (b).

The experimental set-up allows for measurement of the axial and radial stress and the axial deformation. Axial deformation is measured by means of four high pressure LVDTs which are glued in the longitudinal direction on the cylindrical specimens, 90 degrees apart. All experiments are performed in axial deformation control. Loading of the specimens (Fig. 3) occurs by first applying a certain hydrostatic stress. Next, either the radial fluid pressure is kept constant while the axial compressive stress is reduced (load path 1) or the axial compressive stress is kept constant while radial fluid pressure is increased (load path 2). For both load paths, tensile failure of the specimen is obtained, with the fracturing plane perpendicular to the axis of the cylinder.

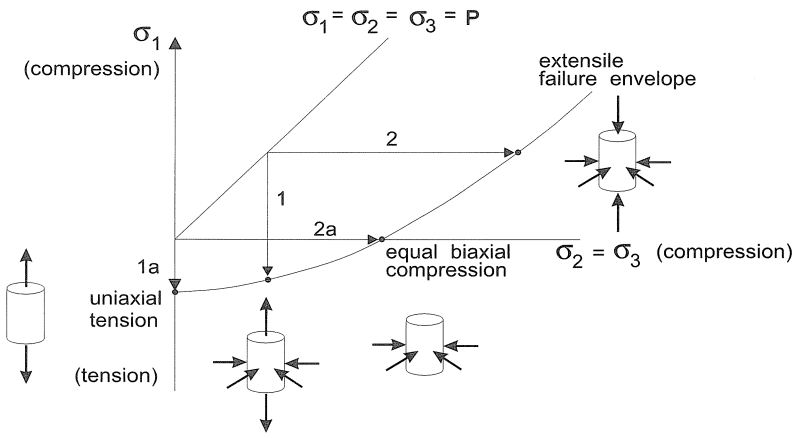

Fig. 3. Load paths investigated in the experiments.

3 Material description

Two materials have been tested in the present research, namely a 2mm mortar and Felser sandstone. The 2 mm mortar consists of aggregates in a matrix of cement, while the sandstone consists of aggregates in a matrix of clay. The composition of the two materials with respect to the aggregate, matrix and pores volume fractions are almost similar. The mortar has an aggregate fraction of about 59%, a cement-matrix fraction of 20.4% and a porosity of 20.6% at the age of testing (42–47 days, Visser, 1997). Felser sandstone has a aggregate fraction of about 58.1%, a clay-matrix fraction of 25.5% and a porosity of 20.4% (Hettema, 1996).

Although the composition of the two materials is very similar, the structure of the two materials is different. Two main differences in structure concern the aggregate-matrix bonds and the pore distribution. The bonding between the aggregates and the matrix in the cement is very poor and the bonds are known to have a lower strength than the bonds in the matrix itself (Hsu, 1963, Mindess, 1989). In addition, the porosity of the bond zone is much higher than in the matrix (Scrivener, 1989). From SEM-pictures, the bonding between the aggregates and the matrix in the sandstone seems much better and the porosity of the bond zone is about similar of that of the matrix (Visser, 1997). Strength differences between the bond and the clay-matrix are not reported but may exist. The pore distribution in the mortar consists of very fine gel pores (<10 nm), capillary pores (10–200 nm) and air bubbles (>200 nm, Neville, 1977). The pores in the sandstone consists of only capillary pores (Visser, 1997). By the lower fraction of capillary pores in the mortar, the permeability of the mortar is much lower than for the sandstone (Visser, 1997).

4 Influence of the degree of saturation

To investigate the influence of the degree of saturation on the behaviour of the two porous materials, uniaxial compression tests on prisms (100 × 100 × 400 mm^3) have been performed. The

mortar has been tested for a degree of saturation of 0% (dry mortar), 69% (unsaturated mortar) and 100% (saturated mortar). The sandstone has been tested for a degree of saturation of 4% (unsaturated sandstone) and 100% (saturated sandstone). The sandstone prisms have been sealed by epoxy resin prior to testing to prevent drainage of the pore water. The mortar specimens are not sealed because water drainage is negligible due to the very low permeability compared to load speed. In the uniaxial compression tests, axial load and axial and radial strains have been measured. To illustrate the results, axial stress-axial strain curves (averages over three tests each) are shown in Fig. 4.

As a general trend, the mortar can be seen to stiffen with degree of saturation while the sandstone weakens. This can be seen even more clearly from the tangent elasticity parameters given in Table 1. The bulk modulus and the shear modulus are calculated by Hooke's law. Both materials show a reduction in compressive strength with increasing degree of saturation, although for the mortar it seems that the compressive strength reduction is important only at high degrees of saturation. The different behaviour of the two porous materials on saturation has to be sought in the influence of the water and water distribution on the materials.

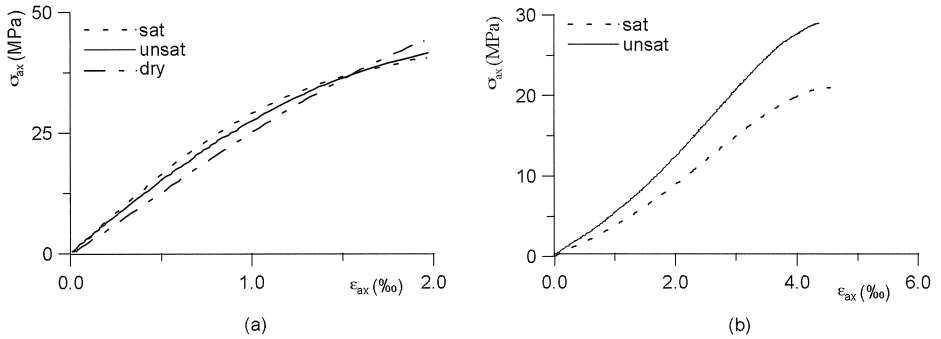

Fig. 4. Axial stress- axial strain curves from uniaxial compression tests on impermeable mortar (a) and sandstone (b).

Table 1. Uniaxial compressive failure stress and tangent elasticity parameters of the uniaxial compression tests.

	Mortar			Sandstone	
	dry (S_r = 0%)	unsaturated (S_r = 69%)	saturated (S_r = 100%)	unsaturated (S_r = 4%)	saturated (S_r = 100%)
F_c (MPa)	52.2 ± 3.5	49.4 ± 3.3	41.6 ± 2.8	29.1 ± 1.1	20.8 ± 0.2
E (GPa)	25.8 ± 0.8	29.7 ± 1.4	32.3 ± 1.2	5.9 ± 0.2	4.4 ± 0.1
v (‰)	0.184 ±	0.210 ±	0.206 ±	0.152 ±	0.183 ±
K (GPa)	0.006	0.007	0.008	0.008	0.009
μ (GPa)	13.6 ± 0.6	17.1 ± 1.0	18.3 ± 1.0	2.8 ± 0.2	2.3 ± 0.1
	10.9 ± 0.5	12.3 ± 0.7	13.4 ± 0.7	2.6 ± 0.1	1.9 ± 0.0

4.1 *Water distribution in porous materials*

The water distribution in porous materials strongly depends on the degree of saturation (Onaisie et al., 1994, Dullien, 1992, Bear and Bachmat, 1991, Wittmann, 1977). At a low degree of saturation ($S_r \approx 0$ to 45 %), the water in the mortar and the sandstone is present only as adhered water. For degrees of saturation between about 0 and 10 %, adhesion takes place mostly *in* laminar cement and clay particles (intra-layer water). At a degree of saturation of 10 to 45%, the adhered water is present also *between* matrix particles (inter-layer water) and as fluid films at free surfaces such as pore walls and microcrack faces (Fig. 5a,b). For degrees of saturation larger than about 45%, the fluid film thickens so that the water in the capillary pore systems become continuous (Dullien, 1992). Stable water-air interfaces are established in the capillary pores (Gregg and Sing, 1981) and this water becomes capillary bonded (Fig. 5c).

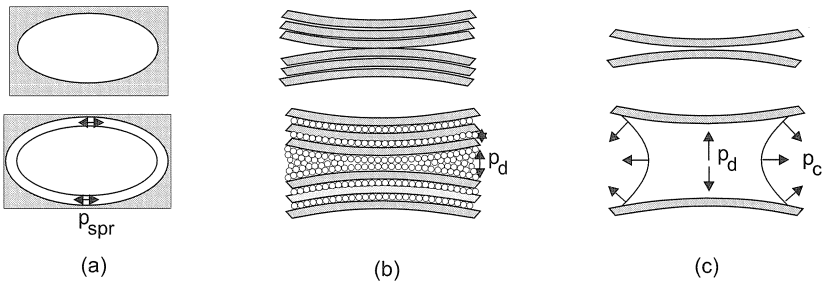

Fig. 5. Spreading pressure p_{spr} in the water film (a), disjoining pressures p_d in the inter-layer and intra-layer water (b) and capillary pressure p_c in the capillary bonded water (c).

Physical adsorption is the result of the forces of attraction and repulsion between the water molecules and the molecules or ions in the solid. The interaction forces are collectively called Van der Waals forces (see for example Israelachvili, 1985). The net force between two particles are sketched in Fig. 6. As a consequence of the higher attraction forces of the water molecules by the solid than the air molecules, the water will adhere to the solid. Thereby it balances partly the attraction forces on the solid surface molecules by the molecules in the interior of the solid, which causes the solid to be in a pre-strained state. Upon partly balancing of the forces on the solid surface molecules (i.e. reduction of the surface tension of the solid), the solid expands. For a water film, it is then said that there exist a so-called spreading pressure (Yates, 1954, see Fig. 5a).
Likewise, there exists a so-called disjoining pressure in the intra-layer and inter-layer water, but since this water is bounded by two solid surfaces, and often charging of the solid interfaces arises, the disjoining pressures are usually much higher than the spreading pressure (Israelashvili, 1985). Although the spreading pressure may have a different magnitude than the disjoining pressure, they both cause swelling of the solid particles and possibly a reduction of strength (Yates, 1954, Hiller, 1963, Mills, 1960, Norish, 1954).

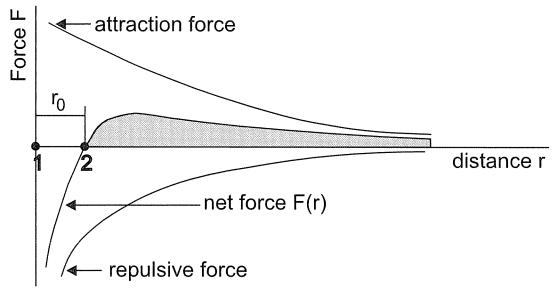

Fig. 6. Attraction and repulsive forces between two molecules or particles (after Mindess and Young, 1981).

For capillary water, a pressure arises due to surface tension at the air/water interfaces (Defay et al., 1966). This capillary pressure given by the air pressure minus the water pressure is always negative. This means that for atmospheric air pressures, the water is in a state of tension. The capillary pressure will decrease the distance between the two particles (Fig. 5c). The unsaturated porous materials will then act like they are compressed by the surface tension of the water (Rossi and Boulay, 1990). With the contraction of the pores by the capillary pressure, disjoining pressures arise also in slits and inter-layers (Powers, 1968, Wittmann, 1977, Mindess and Young, 1981). Above about 95% RH, capillary pressures can be neglected, since the total area of the water/air interfaces (present only in the larger pores) has become too small to have a noticeable effect on the behaviour of the porous materials.

4.2 *The effect of the degree of saturation on mortar*

In the unsaturated mortar (S_r=69%), it is assumed that adhesion of water is maximum and that all micropores are completely water saturated while the capillary pores and air bubbles are unsaturated. Upon uniaxial compressive loading, all water except that in the capillary pores and air bubbles is compressed. Thereby the intra-layer and inter-layer water will give rise to increasing disjoining pressure (Fig. 6). Since the intra-layer water is strongly bonded, it is unlikely that water is squeezed from the cement-particles. In the micropores, by compression of the pore water, compressive pore pressures may be built-up if no water movement to the larger pores occurs. Otherwise, the micropores remain drained (i.e. no pore pressures). The water films in the larger pores will become thicker. The total area of the water/air interfaces reduces as well as the radius of the interfaces, hence the capillary pressure reduces. The pores expand, thereby also reducing the disjoining pressures in wedge-like pores.

Compared to the dry mortar (S_r = 0%), the stiffer behaviour of the unsaturated mortar is then a net effect of three different stresses: increase in disjoining pressure in the intra-layer and inter-layer water, compressive pore pressures in the saturated micropores and decrease in capillary pressures accompanied by a reduction of disjoining pressure in the capillary pores. From preliminary uniaxial tension experiments on the mortar, the air in the impermeable mortar was seen to remain at atmospheric pressure during loading (Visser, 1997). Moreover, the responses of the mortar at a

degree of saturation 69% and 98% are similar. Since for a degree of saturation of 98% capillary pressures are negligible (Reinhardt, 1985), both the capillary pressure and the disjoining pressure induced by the capillary pressure are either negligible or they cancel each other. The stiffer response of the unsaturated mortar compared to the dry mortar is then due to local pore pressures in the micropores and disjoining pressures in the inter-layers and intra-layers. Both pressures counteract the applied uniaxial stress, so that a larger external uniaxial compressive stress has to be applied to maintain a constant deformation rate which means that the unsaturated mortar behaves stiffer.

In the saturated mortar (S_r=100%) also the capillary pores and air bubbles are saturated. Under uniaxial compression, also these pores generate compressive pore pressures counteracting the applied external stress and the saturated mortar responds stiffer than the unsaturated mortar. The increase in stiffness may be either due to the capillary pores alone, or due to both the capillary pores and the micropores. Since the response of the mortar at a degree of saturation of 69% and 98% are similar, the pore pressures in the capillary pores can be built-up only at full saturation. Because air is highly compressible, a small percentage of air is sufficient to give the air/water mixture a high compressibility too (Bear and Bachmat, 1991).

The pore pressures and disjoining pressures can be seen to affect both the volumetric as well as the deviatoric elasticity parameters of the mortar (Table 1), contrary to the general believe that the effect of the pore pressure is volumetric only since pore pressures are hydrostatic (Biot, 1941, 1973). However, the disjoining pressure depends strongly on the orientation of the solid interfaces and thus on the loading direction. By compressing two solid interfaces perpendicular to the direction of loading, repulsive forces increase very fast but for solid interfaces parallel to the direction of loading, attraction forces arise. The attraction forces are much smaller than the repulsive forces. The stiffening in the axial direction will then be larger than in the lateral direction, even for isotropic materials. Therefore, both the lateral and axial deformation of the unsaturated mortar will be less than for dry mortar, as can be seen from the increase in Young's modulus and shear modulus. Since the decrease of the axial deformation is largest, the Poisson's ratio increases as well. Because of the similarity of the Poisson's ratio of the unsaturated and saturated mortar, the effect of the (hydrostatic) pore pressures on the deformation is *NOT* similar for the three directions.

The difference between the uniaxial compressive failure strength of the dry and unsaturated mortar is negligible. The saturated mortar has however a much lower compressive strength than the unsaturated and dry mortar. Compressive strength reduction upon saturation is an often reported phenomenon, and seems to be caused by two effects: a local strength reduction (i.e. loss of cohesion) upon adhesion of the intra-layer and inter-layer water and the compressive pore pressures. The adhesion of intra-layer and inter-layer water is largely completed above a degree of saturation of 45%. Because the compressive strengths of the dry mortar and the unsaturated mortar are approximately similar, the local strength reduction upon saturation seems to be negligible. Hence, the low uniaxial compression failure stress of the saturated mortar is caused exclusively by the compressive pore pressures in the capillary pores. A more detailed explanation will be given in Section 6.

4.3 *The effect of the degree of saturation on sandstone*

The behaviour of the sandstone with degree of saturation is opposite to that of the mortar: upon saturation the material weakens. The only possible explanation for this behaviour is that although disjoining pressures and pore pressures likely lead to an apparent stiffening of the sandstone, the reduction of the cohesion of the sandstone by the water is dominant. By the presence of the water in and between the clay particles, not only the bond stiffness of the saturated mortar decreases, but also the internal friction in and between the clay particles which facilitate shearing on the inter-layers and intra-layers of the clay. Hence, the elasticity parameters of the saturated sandstone are lower than those of the unsaturated sandstone.

The saturated sandstone has a much lower uniaxial compressive failure strength than the unsaturated materials. Part of the strength reduction may be caused by the loss of strength of the sandstone upon saturation, as was argued from the weakened deformational behaviour. From uniaxial compression tests performed by Hettema (1996), the dry sandstone compressive failure strength is as high as 35.9 MPa, compared to 30.5 MPa for the unsaturated specimen. Considering the minor difference in degree of saturation, this strength reduction is remarkable. At a saturation degree of 4%, the reduction of strength upon saturation is not yet maximum, since only intra-layer water is likely to be present, while also inter-layer water and water films are known to be able to reduce the cohesion of materials (Amanullah et al., 1994). Hence, the low uniaxial compressive failure strength of the saturated sandstone compared to the uniaxial compressive failure strength of the unsaturated sandstone can be expected to be partly due to loss of material strength, partly due to pore pressure effects.

5 Dry fracturing

Dry fracture experiments are performed on impermeable unsaturated sandstone. In the dry fracture experiments, the cylindrical specimens tested in the Hookean cell are sealed and sleeved so that no water from the reservoir of the cell can penetrate the sandstone or the fracture. O-rings are placed in the notch to prevent the sleeve to be pushed into the notch. For the constant radial stress load paths (i.e. load path 1 in Fig. 3), experiments are performed for the uniaxial tensile load path (constant radial stress is zero) and at a constant radial stress of 1, 2, 3, 4, 6 and 8 MPa. For the constant axial stress load path, experiments have been run on constant axial stresses of 0 MPa only (biaxial compression tests). Higher constant axial stress tests could not be performed because the cell could sustain pressures up to 100 MPa only, the radial failure stresses being much higher than that for non-zero axial compressive stress. The response curves in this section are from single tests.

5.1 *Uniaxial tension test*

The response curve of a uniaxial tension test on the impermeable unsaturated sandstone is shown in Fig. 7a. At the onset of the deformation, the general response of the material will be a tensile axial deformation with increasing stress (stage 1). The enlargement of the response curve in Fig. 7b shows that the response is linear at first (stage 1a), but becomes increasingly nonlinear prior to reaching the

maximum tensile stress (stage 1b). For the quasi-brittle materials under consideration, the general nonlinear response is mostly due to microcracking.

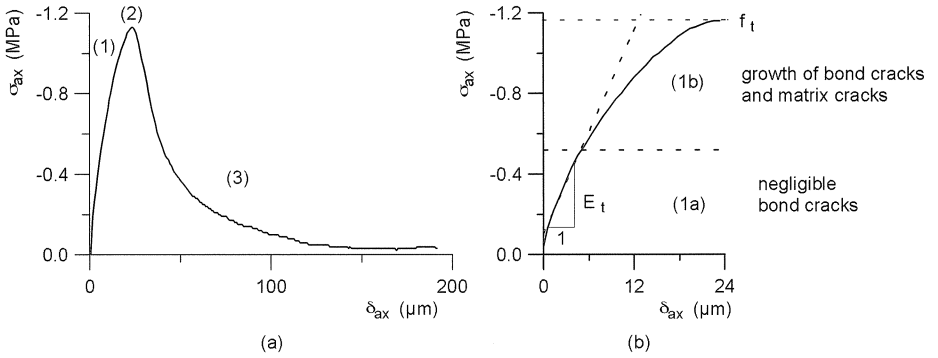

Fig. 7. Response curve of a dry uniaxial tension test on the unsaturated sandstone (a) and enlargement of pre-peak response (b).

Microcracks will arise at the weakest points in the material, usually in the bond zone between the aggregates and the matrix material and at the entrapped pores (e.g. Hsu, 1963, Petersson, 1981, Arslan et al., 1995). At low stresses, first the bonds parallel to the maximum tensile stress will fail. With increasing stress, also bonds not parallel to the uniaxial tensile stress and matrix bonds begin to fail. With the increase in microcracks and the related weakening of the material, less stress must be applied to maintain a constant deformation rate. The response curve then becomes increasingly nonlinear, until the maximum stress bearing capacity of the material has been reached, i.e. the response curves reach the maximum tensile stress the specimen can sustain (stage 2 in Fig. 7a). At the peak stress, it is usually assumed that a (macro-) fracture is initiated due to the linking and extension of the microcracks. The maximum uniaxial tensile stress is then defined as the tensile strength of the mortar. It should be mentioned that the definition of the maximum tensile stress as the fracture initiation stress is an ill defined point. The major fracture may well be initiated either before or after peak (Hordijk et al., 1989).

Beyond the peak (Fig. 7a, stage 3), the materials are characterized by a decrease in stress at an increasing deformation, until complete material failure. This so-called softening behaviour is due to the decrease of the stress-bearing capacity of the material. The decrease in stress bearing capacity, characteristic for all quasi-brittle materials, is mainly due to progressive microcracking and fracture propagation by subsequent linking and extending of microcracks with the fracture at increasing deformation. Based on the experimental observations of fracturing of quasi-brittle materials, there seems to be reached a general consensus in concrete, rock and ceramic mechanics that the so-called cohesive fractures in quasi-brittle materials consist of a "real" or stress free crack, preceded by a zone of crack face bridges through which stresses still can be transmitted and possibly a zone of microcracking (Fig. 8, Van Mier, 1991, 1992). The microcrack zone and the bridging zone together

are called the cohesive or process zone. The fracture tip is usually taken as the end of the cohesive zone, hence there is no well defined crack tip. Fracture propagation will occur when progressive failure of the material will cause the stress-free fracture to extend.

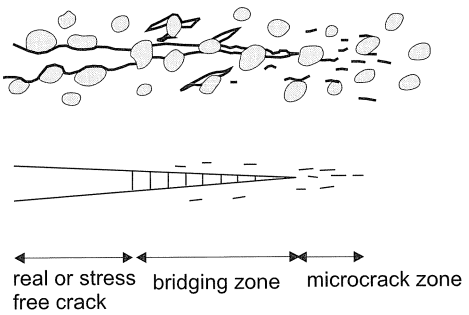

Fig. 8. Cohesive fracture model.

The above meso-mechanical description of the response of the sandstone under uniaxial tension states the three main stages of the fracture problem: deformation of the material represented by the pre-peak response, fracture initiation represented by the peak of the response and fracture propagation represented by the post-peak response. These three stages are however not very well separated as was already shown for fracture initiation.

5.2 *Biaxial compression test*

The response curves of the biaxial compression tests on the impermeable unsaturated sandstone are shown in Fig. 9b. For comparison, the response curves of the uniaxial tension tests are shown in Fig. 9a as well.

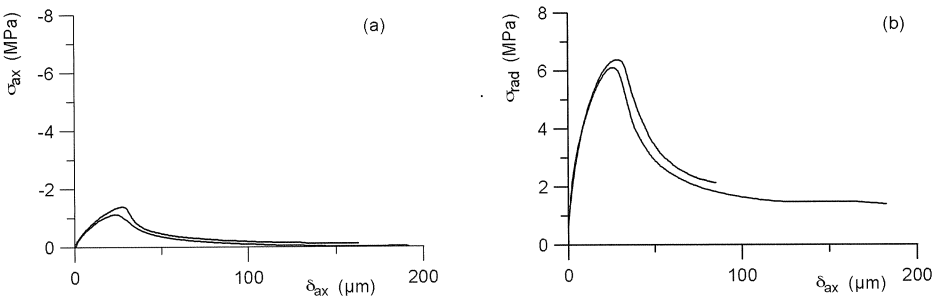

Fig. 9. Response curves of dry uniaxial tension (a) and biaxial compression (b) tests on the unsaturated sandstone.

Although for both the uniaxial tension tests and the radial compression tests the specimens fail in tension at the macro-level with the fracturing plane perpendicular to the axial of the cylinder, several differences can be noted. The main differences in response are a smoother and much broader peak, a higher failure stress and a higher tail of the radial compressive stress response. These difference can be explained by the way stresses are transmitted through the sandstone and the microcracks are distributed. The stress transfer in the sandstone is illustrated in Fig. 10. Under uniaxial tension at the macro-level, local tensile stresses arise. When the local tensile stresses are larger than the local strengths in the material, microcracks are generated. The microcracks are genenerated mostly at the cement-aggregate bonds, being the weakest link in the sandstone (Fig. 10a). Under biaxial compressive stress at the macro-level, the local tensile forces in the biaxial stress plane are very small or even absent, by balance of the two equally large compressive forces in the two directions. In the axial direction, the stress situation is depicted in Fig. 10b. Local tensile stresses and bond cracks are generated in the material at the aggregates by the out-of-plane transmission of the local compressive forces at the aggregate contacts (this follows directly from equilibrium considerations). Hence, since the local tensile stresses are much smaller under biaxial compression, a higher external biaxial stress has to be applied to initiate microcracks.

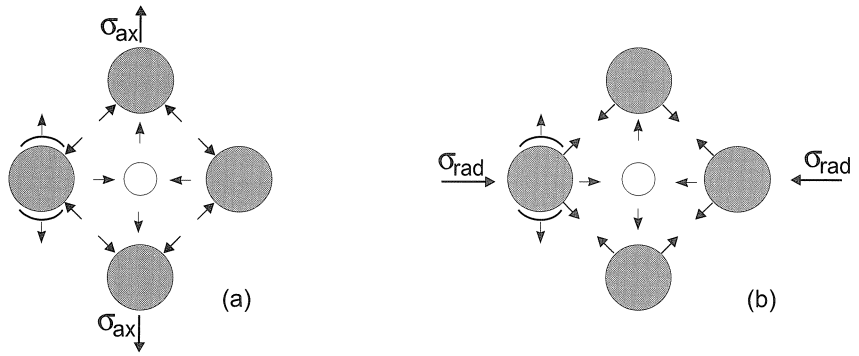

Fig. 10. Local stresses and bond cracks under uniaxial tension (a) and biaxial compression (b) applied at the macro-level.

The ratio of biaxial compressive failure stress over uniaxial compressive failure stress f_{bc}/f_{uc} =0.2 for sandstone which is low compared to the ratio of 1.2 often reported for concrete (Kupfer, 1973). On the other hand, Newman (1978) reported a f_{bc}/f_{uc} ratio of 0.2 as well. It is not certain if the ratio is truly very low or that there is a stress transfer at the vertical faces at the notch. Although the O-rings are placed in the notch to prevent the sleeve from being pushed into the notch, this may not be completely prohibited. If the sleeve is just slightly pushed into the notch, it may introduce an axial tensile splitting stress, stimulating fracture initiation. A further discussion of the vertical notch face loading is delayed to Section 6.

5.3 *Triaxial extension tests at a constant radial stress*

Relative response curves (one for each load-path) of the triaxial tests on a constant radial stress are given in Fig. 11. The curves are given relative to the deformation and stress after initiation to the prescribed hydrostatic stress.

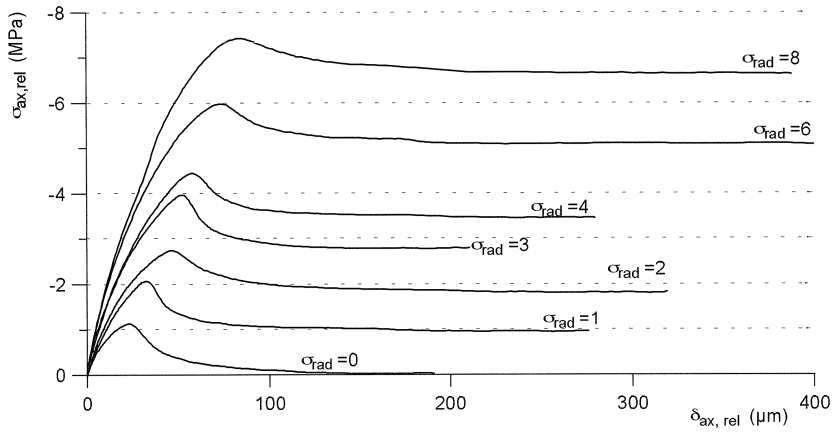

Fig. 11. Relative response curves for the constant radial load path for dry fracturing of impermeable unsaturated sandstone.

The relative response curves show an increase in stiffness of the pre-peak response, progressively higher relative axial failure stresses and residual stresses (i.e. magnitude of the tail of the responses) with increase in radial compressive stress. These observations, both in extensile and compression failure, are typical for quasi-brittle materials (e.g. Jamet et al., 1984, Newman, 1978, Gowd and Rummel, 1980, Scott and Nielssen, 1991, Handin and Hager, 1957).

The increase in stiffness of the sandstone with increase in constant radial stress can be explained by the non-linear deformation behaviour of the sandstone under hydrostatic compression. The highly nonlinear deformation behaviour of the sandstone is caused both by inelastic behaviour such as microcracking and pore collapse (Walsh, 1965), but also by (elastic) change in contribution of the different constituents of the sandstone to the overall deformation. The dry material deformation will at first instant be determined mostly by the pore compressibility, since the (air-filled) pores are the most compressible constituent. With increasing hydrostatic stress, the contribution of the matrix and aggregate to the deformation increases (Schatz, 1976). Since the aggregates are stiffer than the pores and matrix, the overall response of the sandstone becomes stiffer. Upon reduction of the axial compressive stress after the hydrostatic loading, the response is still much stiffer for the high confining stress tests, on account of the higher contribution of the aggregate fraction to the deformation (Newman, 1978).

The influence of the radial stress on the axial failure stress is given in Fig. 12, which shows the failure stresses of all dry fracture experiments performed. In the figure, it can be seen that the contribution of the radial stress to failure is about one fourth of that of the axial stress. The smaller contribution of the radial stress is a consequence of the small local tensile stresses generated by the radial compressive stress, as discussed in Section 5.2. The linear relationship is however surprising and may be a consequence of the small stress range under consideration or of the notch loading, as discussed in Section 5.2. In Fig. 12, also the biaxial compressive failure stress is given. As can be seen there is no load path dependency.

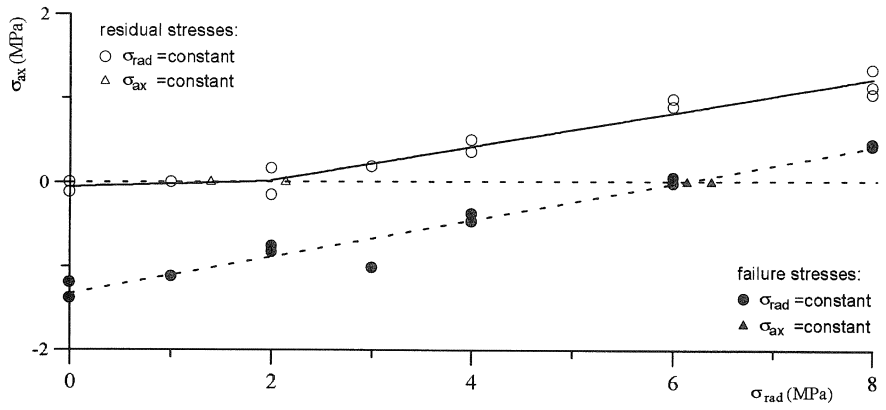

Fig. 12. Extensile dry failure envelope for the unsaturated sandstone.

The reduction of stress bearing capacity of the sandstone after the peak stress is reached, is very modest (Fig. 11). The residual strengths (i.e. the level of the tails of the response curves) are given in Fig. 12. The radial compressive stress becomes important for fracture propagation when it is larger than 2 MPa. For lower radial compressive stresses, the residual axial stress decreases to zero at maximum crack opening. For a constant radial stress of 2 MPa, the residual axial stress becomes compressive so the residual radial stress has to contribute as well. The increase in residual axial stress with residual radial stress is almost similar to the increase in axial failure stress with radial failure stress. Also no load path dependency for the fracture propagation stresses is found.

6 Hydraulic fracturing of impermeable mortar

Hydraulic fracture experiments of impermeable porous materials are performed on impermeable unsaturated and saturated mortar. In these hydraulic fracture experiments, oil is used as reservoir fluid in the Hookean cell to which the mortar is impermeable. The impermeability refers to the fracture fluid rather than to the pore fluids. The surface of the specimens (but not the notch) are completely sealed by epoxy resin to fill surface pores which might act as fracture initiators.
The impermeable unsaturated and saturated mortar are tested for a constant radial stress of 0, 2, 4, 6 and 8 MPa and for a constant axial stress of 0, 2 and 4 MPa. The response curves in this section are from single tests.

6.1 *Uniaxial tension test*

The response curves of the uniaxial tension tests on the impermeable unsaturated and saturated mortar are shown in Fig. 13. Because the radial fluid pressure in these tests is zero (although the cell is filled with oil), the fluid pressure in the notch of the specimens as well as in the fracture is zero.

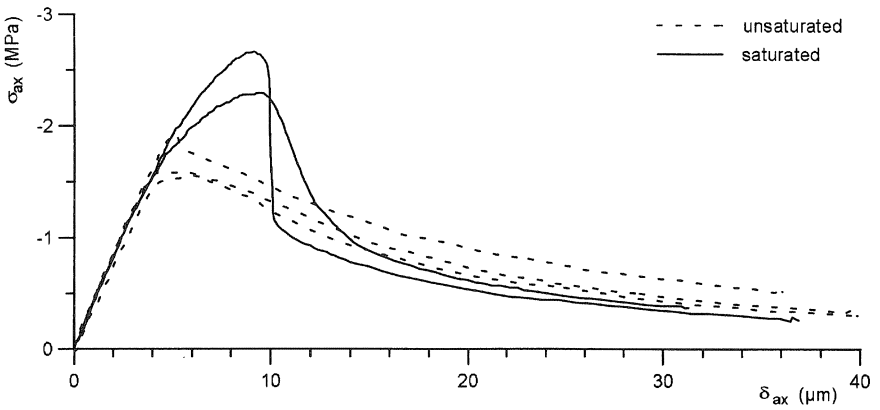

Fig. 13. Response curves of uniaxial tension tests on the impermeable mortar.

The tangent Young's modulus of the saturated mortar (average 32.3 GPa) are just slightly higher than that of the unsaturated mortar (average 29.8 GPa). This difference is about similar as found from the uniaxial compression tests (Section 4). As discussed, the stiffer response of the saturated mortar is caused by the pore pressures in the capillary pores. In the uniaxial tension tests, the pore pressure is tensile, since upon elongation of the specimen, the (pore) volume of the specimen increases so that the water in the pores has to spread over a larger volume. The tensile pore pressure counteracts the applied uniaxial tensile stress and a higher uniaxial tensile stress has to be applied to maintain a constant deformation rate.

In addition to the stiffer response of the saturated mortar upon loading compared to the unsaturated mortar, the uniaxial tensile failure stress of the saturated mortar (-2.8 MPa) is much higher (i.e. more tensile) than that of the unsaturated mortar (–1.8 MPa). The difference in uniaxial tensile failure stress may be caused by two local effects: a local strength increase or a local stress increase. Local strength increase of the saturated mortar compared to the unsaturated mortar is unlikely to occur. First of all, the general influence of the water is a strength reduction, rather than a strength increase, because the water reduced Van der Waals forces (Section 4). Moreover, because of the high degree of saturation of the unsaturated mortar, weakening effects from the water are expected to be approximately similar in the two types of mortar. The apparent strength increase of the saturated mortar is thus most likely caused by a change in local stresses. The difference in local stresses, and their effect on the apparent local strength of the mortar are schematized in Fig. 14.

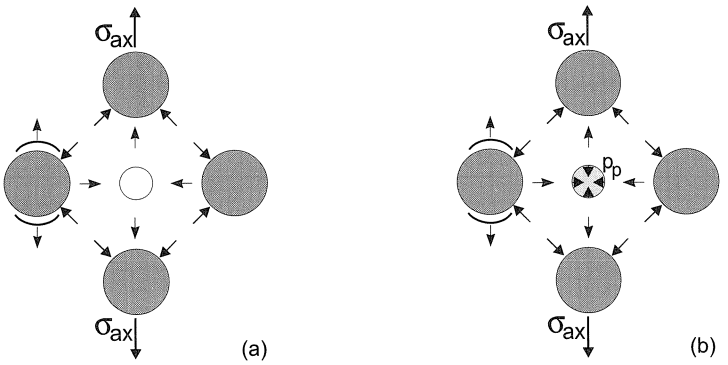

Fig. 14. Local stresses and effect of the pore water on the impermeable unsatured mortar (a) and the saturated mortar (b) under uniaxial tension applied at the macro-level.

In uniaxial tension, the main local crack mode for both the unsaturated and the saturated mortar will be pull-apart of the bonds. However, the tensile pore pressure in the saturated mortar counteracts the tensile stress and thus reduces the local tensile stress. Therefore, a higher tensile stress has to be applied in order to initiate microcracks. Moreover, with progressive microcracking the pore water has to spread over a larger volume and the tensile pore pressure will increase. Linking and extension of the microcracks will therefore occur at a higher stress than for the unsaturated mortar.

After reaching the maximum tensile stress, the response curve of the impermeable saturated mortar drops almost instantaneously after which the stress for propagating the fracture is much lower than for the unsaturated mortar (Fig. 13). The response curve of the unsaturated mortar shows a more gradual decrease in uniaxial stress after reaching the uniaxial failure stress. The difference in behaviour of the two types of mortar after peak stress may be caused by different local phenomena. A first explanation derives from possibly different fracture tip pressures. After initiation, the fracture oil is free to enter the fracture. However, the fracture oil is at atmospheric pressure in these uniaxial tensile tests. Because of the surface tension of the highly viscous oil (about 70 times as high as that of water), the oil cannot penetrate the whole fracture. A non-penetrated fracture zone, called fluid lag, will therefore exist at the fracture tip (Fig. 15, Ingraffea et al., 1995).

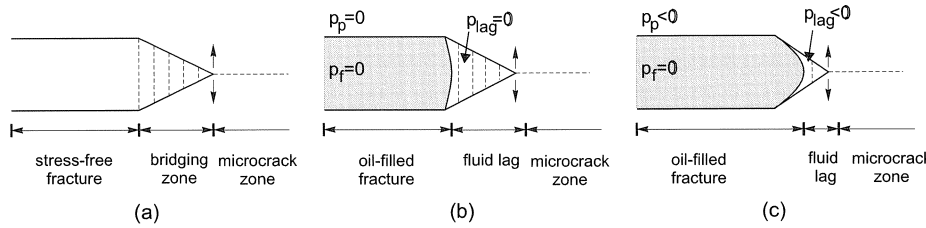

Fig. 15. Cohesive fracture models for a dry fracture (a), a hydraulic fracture in the unsaturated mortar (b) and in the impermeable saturated mortar (c).

The length of the oil lag is to first order determined by the capillary pressure between the fracture oil and the fluid in the fracture tip. This means that the lag is dependent on the pressure difference between fracture oil and oil lag fluid and the aperture of the fracture (Ingraffea et al., 1995). In the unsaturated mortar, the fluid in the oil lag region is most likely air (at atmospheric pressure). The fracture then must have already a large opening before the fracture oil will penetrate the fracture. In the saturated mortar, where no air is present, it is unlikely that water will flow to the fracture tip, because the permeability of the mortar to the water is low and because the water in the saturated mortar is already tensioned. The pressure in the oil lag region will be at vacuum (Nilson, 1981) or close to it. By the evacuated fracture tip, the oil lag in the saturated fracture can be expected to be much smaller than in the unsaturated mortar. As a result of the smaller fluid lag in the saturated mortar, the bridging zone of the hydraulic fracture in the saturated mortar is expected to be smaller than in the unsaturated mortar (Fig. 15). Since the bridges no longer can transfer stress, a lower uniaxial tensile stress on the specimen is required to propagate the fracture and the softening branch of the saturated mortar is then lower than for the unsaturated mortar.

It is not clear if such a dominant difference in crack tip pressures between the unsaturated and saturated mortar exists. Once a fracture is created, the material neighbouring the fracture will relax and the tensile pore pressures will reduce. Pore water then may flow to the fracture tip. It is unclear what causes the lower residual stress for the saturated mortar.

6.2 *Biaxial compression tests*

The response curves of the biaxial compression tests on the impermeable unsaturated mortar and saturated mortar are shown in Fig. 16b. For comparison, the response curves of the uniaxial tension tests on the impermeable unsaturated and saturated mortar are shown in Fig. 16a as well.

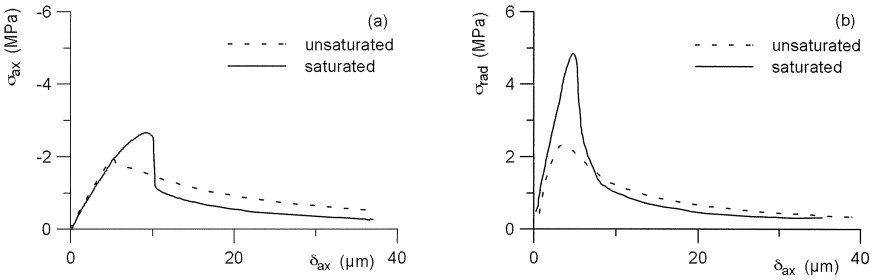

Fig. 16. Response curves of the hydraulic uniaxial tension tests (a) and hydraulic biaxial compression tests (b) on the impermeable mortar.

In Fig. 16b, it can be seen that the saturated mortar has a much higher apparent Young's modulus than the unsaturated mortar. Using the Poisson's ratio's obtained from the uniaxial compression tests (Table 1), the Young's moduli of the unsaturated and saturated mortar are similar to those obtained from the uniaxial tensile tests. Since in the biaxial compression tests the notch is

pressurized, it can be concluded that the effect of the pressure on the notch faces has little influence on the elasticity parameters of the mortar.

The biaxial compressive failure stress is much higher for the saturated mortar than for the unsaturated mortar. The effect of the degree of saturation on local failure of the unsaturated and saturated mortar is schematized in Fig. 17. As already discussed for the uniaxial tensile tests, the effect of the water on the local strength of the saturated material is unknown, but likely not very strong (compared to both the dry and unsaturated mortar). More important is the local stress distribution in the material. Under biaxial compression, the local stresses in the saturated mortar are much lower than in the unsaturated mortar. This local stress reduction is partly caused by transition of the stresses through the compressed pore water, partly because the pore pressure prohibit aggregate contacts to establish. Thus, local tensile stresses by wedging of grains can not take place as easily as in the unsaturated mortar. Microcracking does not occur until very high biaxial compressive stresses are applied. This can also be seen from the response curve in Fig. 16, where it is shown that the saturated mortar behaves almost linear up to the peak stress. This indicates that microcracking prior to fracture initiation is (almost) absent.

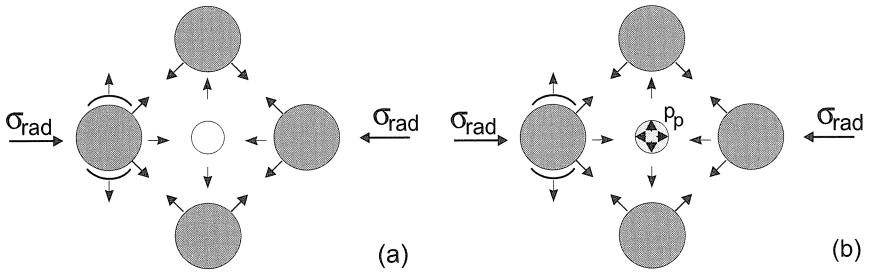

Fig. 17. Local stresses and effect of the pore water on the impermeable unsaturated mortar (a) and saturated mortar (b) under biaxal compression applied at the macro-level.

Although the above local failure mechanisms may explain the difference in biaxial failure stress between the unsaturated and saturated mortar, it should be noted that the biaxial compressive failure stress for the unsaturated mortar is (except for the sign) as large as the uniaxial tensile failure stress. This is highly remarkable since it is expected that the unsaturated mortar has about the same failure stress as the dry mortar, i.e. the water in the unsaturated mortar has only a minor influence on the failure stress. In Section 5, on the other hand, it was shown for sandstone that the biaxial compressive stress in *dry fracturing* can be expected to be much higher than the uniaxial tensile failure stress. The effectiveness of the radial stress to generate local tensile stresses causing micro-cracking and initiation of a macrofracture is then much lower than the effectiveness of the uniaxial tensile stress (about a factor four was found for the sandstone). The low biaxial compressive stress for the unsaturated mortar can then be expected to be a consequence of the *hydraulic fracturing*. The hydraulic fracture initiation in the unsaturated and saturated mortar is illustrated in Fig. 18.

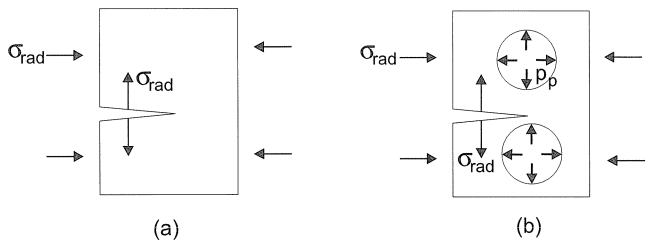

Fig. 18. Effect of the pressure in the notch for the unsaturated mortar (a) and the saturated mortar (b) under biaxial compressive stress.

In Fig. 18a, failure for the unsaturated mortar under biaxial compression is shown. For hydraulic fracture initiation in the impermeable mortar, the fracture oil in the notch will impose a pressure on the crack faces. This crack face pressure gives rise to tensile splitting forces. By the similarity of the uniaxial tensile failure stress and the biaxial compressive failure stress, it seems that the notch pressure is the dominant stress causing fracture initiation in the unsaturated mortar. However, it is likely that also the radial compressive stress contribute to the failure. The exact contributions of the two stresses can however not be deduced from these tests.

The effect of the notch pressure can be expected to be much less in the saturated mortar than in the unsaturated mortar. This is illustrated in Fig. 18b. Due to the counteracting pore pressures, the compressive stress can be said to be less effective in generating local tensile stresses in the mortar, as explained above. But the pore pressures will also have the same counteracting effect on the notch pressure. The reduction in effectiveness of both the radial compressive stress and the notch stress may explain the much lower ratio of biaxial compressive failure stress of the unsaturated mortar and the saturated mortar compared to the ratio of the uniaxial tensile failure stresses.

In Fig. 16, it can be seen that the tails of the response curves for the unsaturated and saturated mortar are almost similar, even though the saturated mortar has much higher failure stress. Since the radial fluid pressure is not zero, the pressurized oil in the crack will impose an extra body force normal to the fracture walls. In addition, the fluid lag in the fracture will be lower than for the uniaxial tension test. Yet for the highly viscous fracturing oil, a fluid lag will likely still exist. At the fracture tip, the pressure is either atmospheric (unsaturated mortar), or tensioned or vacuum (saturated mortar). The pressure in the fracture then has to drop from its maximum pressure at the fracture opening to the pressure at the fluid lag boundary. It is known that for the quasi-static fracture propagation, the pressure in the fracture is fairly constant and most of the pressure drop will occur at the fluid lag boundary (Desroches and Thiercelin, 1993). The fluid pressure on the fracture faces serves as an additional tensile splitting force and will stimulate fracture propagation. The smaller the fluid lag, the more effective the fracture pressure will be. Moreover, the fracture pressure will give rise to wider fractures than in the dry fracture case. This will lead to a smaller

bridging zone for the fluid filled fractures, causing the mortar to behave more brittle (Brühwiler and Saouma, 1991).

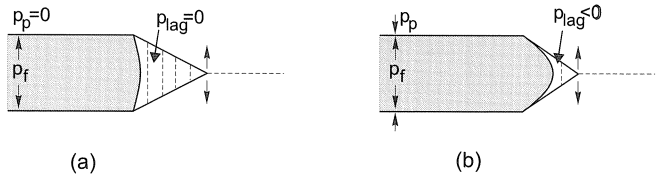

Fig. 19. Cohesive fracture models for a pressurized hydraulic fracture in the impermeable unsaturated mortar (a) and in the impermeable saturated mortar (b).

The fracture pressure is likely less effective in propagating the fracture in the saturated mortar than in the unsaturated mortar, as a result of counteracting pore pressures. The tail of the response curves for the unsaturated and saturated mortar are however similar. From the uniaxial tensile tests, it was observed that the saturated mortar needs a lower stress to propagate a fracture. The similarity of the tails of the response curves in the biaxial compressive tests then indicates that the fracture pressure is less effective in propagating the fracture. This is caused by the pore pressures in the neighbouring mortar which counteract the fracture pressure (Fig. 19b). Due to the fluid lag, the fracture pressure does not directly influence the stresses at the fracture tip.

6.3 *Triaxial extension tests*

The response curves of the triaxial extension tests at a constant radial compressive stress (load path 1 in Fig. 3) on the impermeable unsaturated and saturated mortar are given in Fig. 20. The response curves of the triaxial extension tests at a constant axial compressive stress (load path 2 in Fig. 3) on the impermeable unsaturated and saturated mortar are given in Fig. 21.

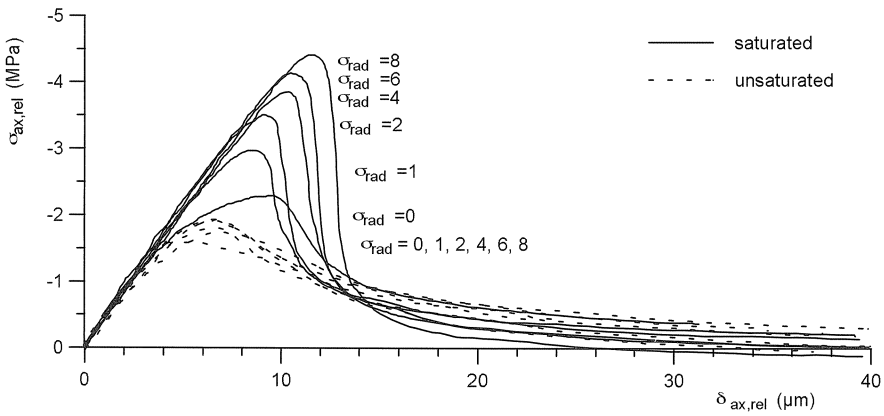

Fig. 20. Relative response curves for hydraulic fracture tests at a constant radial stress on the impermeable mortar.

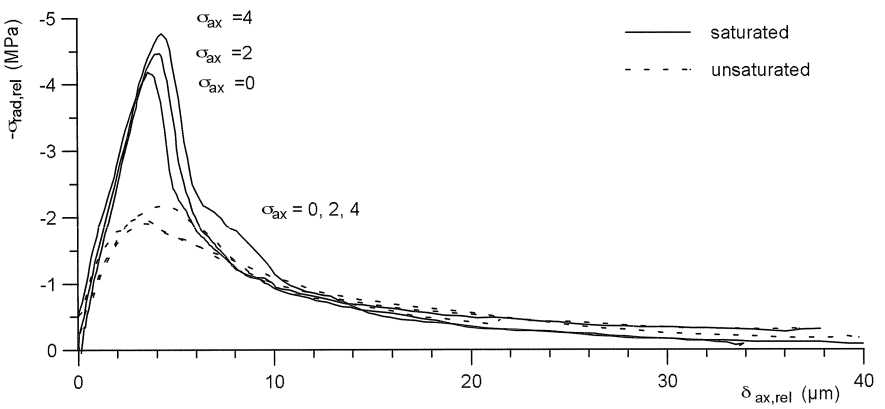

Fig. 21. Relative response curves for hydraulic fracture tests at a constant axial stress on the impermeable mortar.

Comparison of the response curves of the different constant radial stress tests indicate that the response curves of the unsaturated mortar are more or less independent of the constant radial stress. For the tails of the responses, however, the residual stress decreases with increasing constant radial stress. For the saturated mortar, the response curves show that the initial linear response is approximately constant. Also the nonlinear response prior to the peak is constant, except for the tests at a constant radial stress of 0 and 1 MPa. The failure stresses increase with constant radial stress whereas the tails increase with increasing constant radial stress. Comparison of the response curves of the different constant axial stress tests indicate that the response curves of the unsaturated mortar are independent of the constant axial stress, including the tails of the responses. The response curves of the saturated mortar are also more or less independent of the constant axial stress, except for the failure stresses and the stress drop just after peak.

The tests show that the hydrostatic stress has no influence on the linear elastic behaviour of both the unsaturated and the saturated mortar, contrary to what was found for the sandstone (Section 5). The influence of the hydrostatic stress on the failure stresses of the mortar is shown in Fig. 22, which shows the failure stresses of all hydraulic fracture experiments performed on the impermeable mortar. In the figure, it can be seen that for the unsaturated mortar the contribution of the radial stress to failure is similar to that of the axial stress. However, for the saturated mortar, the contribution of the radial stress is lower. For comparison, also the dry failure envelope for the sandstone is shown.

Although the behaviour of the unsaturated mortar and unsaturated sandstone may be different, it is expected, from other dry fracturing experiments on mortar (e.g. Newman, 1978), that the dry failure envelope of the mortar shows a similar low contribution of the radial stress to failure. Part of the contribution of the radial failure stress to failure is then due to the notch, as explained in Section 6.2 (see also Fig. 18). The lower contribution of the radial stress to fracture initiation in the saturated

mortar is due to pore pressures. The pore pressures have a larger effect on the radial stress than on the axial stress or notch pressure by the biaxial nature of the radial stress (Section 6.2). The unknown contribution of the notch pressure to fracture initiation and the pore pressures cannot be deduced from lack of dry fracture data on the impermeable mortar. Moreover, the increasing failure stresses of the saturated mortar are difficult to relate to the lower uniaxial compressive failure stress of the saturated mortar compared to the unsaturated mortar. In the uniaxial compression tests, the saturated mortar possibly fails under a biaxial tensile stress generated by the pore pressures in the direction perpendicular to the applied stress. However, a different local failure mode by pore fluid wedging is possible as well.

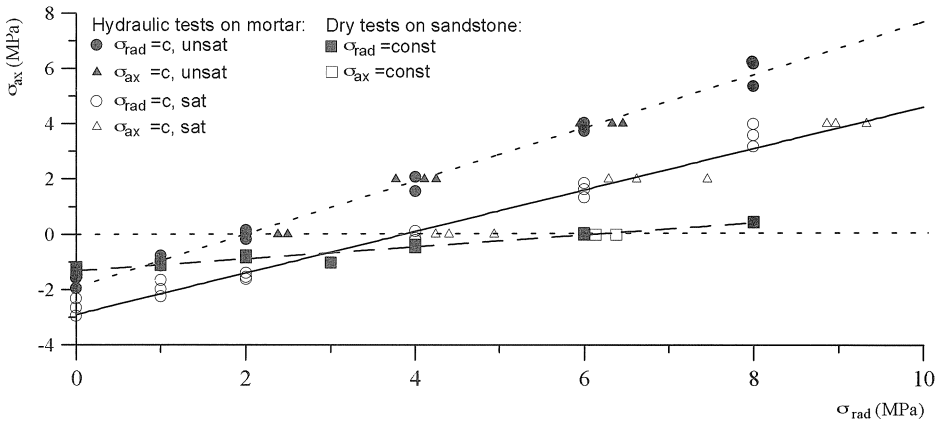

Fig. 22. Extensile dry and hydraulic failure envelope.

The most remarkable difference between the response curves of the hydraulic fractured mortar (Fig. 20, 21) and the dry fractured sandstone (see Fig. 11), is that the relative residual stress of all hydraulic fracture experiments on mortar is close to zero. Thus the residual stresses are all close to the hydrostatic stress at the onset of the experiments. This is contrary to the dry fracture tests on sandstone where the residual stress is only slightly lower than the (axial or radial) failure stress. From extensile tests on mortar (Newman, 1978), it is known that mortar has similar high residual stress as the sandstone in dry fracturing. The fracture pressure thus contributes so much to the fracture propagation that only a little differential stress (axial stress minus radial stress) is needed to propagate the fracture. Consequently, the stress bearing capacity of the mortar is greatly reduced. The hydrostatic stress has a negligible influence on the propagation of the hydraulic fracture and the mortar remains brittle for the hydrostatic stress range tested.

7 Conclusions

Uniaxial compression tests showed that the response of the 2 mm mortar is dependent on the degree of saturation. The response of the saturated mortar was concluded to differ from the unsaturated mortar by the effect of the pressures in the capillary pores and possibly also in the micropores. These pore pressures counteract the applied stress, giving the saturated mortar a stiffer response than the unsaturated mortar. The Poisson's ratio of the saturated mortar is similar to that of the unsaturated mortar, indicating that the effect of the pore pressures is not hydrostatic, as is usually assumed in poroelastic theory (Biot, 1941). The tangent elasticity parameters of the unsaturated and saturated mortar are independent of load direction and the hydrostatic stress range of 0 to 8 MPa.

The uniaxial compressive strengths of the dry and unsaturated mortar are approximately similar, indicating that disjoining pressures and capillary pressures in the unsaturated mortar likely have a negligible influence on the strength of the mortar. The uniaxial compressive strength of the saturated mortar is lower than that of the unsaturated mortar. On the other hand, the uniaxial tensile strength of the saturated mortar is higher than that of the unsaturated mortar. This indicates that the (tensile) pore pressures reduce the effectiveness of the uniaxial tensile stress to initiate a fracture. The lower compressive strength for the saturated mortar seems to contradict the simple superposition rule that the pore pressures counteract applied stresses and thus increase the failure stresses. In the directions perpendicular to the applied uniaxial compressive stress, however, a biaxial tensile stress state prevails. This causes the saturated mortar to fail at a lower uniaxial compressive stress.

From dry extensile fracturing experiments on unsaturated sandstone it was found that the contribution of the radial compressive stress to dry fracture initiation is about one fourth of the axial stress. A similar moderate contribution is also expected for the unsaturated mortar, although the exact contribution is unknown. From hydraulic extensile fracturing experiments on unsaturated mortar, the contribution of the radial compressive stress was found to be as large as that of the axial stress. The large contribution is mostly due to the pressure in the notch which serves as an additional axial splitting stress. From hydraulic extensile fracturing experiments on saturated mortar, pore pressures counteract both the applied axial stress and the radial stress, thereby increasing the tensile strength of the mortar. The effect of the pore pressure is larger on the radial compressive stress, by the two-dimensional nature of the radial stress. Consequently, the contribution of the radial compressive stress to failure of the saturated mortar was found to be smaller than to failure of the unsaturated mortar. The exact contribution of the notch and the pore pressure effect could not be deduced because of lack of dry fracture data on the impermeable mortar. Load path dependency in the extensile failure regime is absent.

After initiation of the hydraulic fracture at the peak of the response curves, only a small deviating stress from the hydrostatic stress, at which the tests are started, is needed to propagate the fracture. From the dry fracture experiments on the sandstone, it was shown that for dry fracturing a stress just slightly different from the failure stress is needed to propagate the fracture. A similar behaviour in dry fracturing is expected for the mortar. The strong difference in residual stress in the dry and

hydraulic fracture experiments is due to the fracture pressure. The fracture pressure seems to dominate the fracture propagation, especially at high hydrostatic stresses. The behaviour of the mortar thus remains brittle, even at high hydrostatic stresses. The residual stresses for the unsaturated mortar and the saturated mortar are almost similar. From the uniaxial tensile tests, it was found that the saturated mortar require less stress to propagate the fracture, possibly due to the smaller fluid lag in the fracture by which the stress transferring capacity of the fracture in the saturated mortar is reduced. Higher fracture pressures are however needed to propagate the hydraulic fracture in the saturated mortar under biaxial or triaxial loading, since the pore pressures reduce also the effectiveness of the fracture pressure. The effects of the smaller fluid lag and pore pressures together then seem to be negligible.

8 Acknowledgements

The authors would like to thank Mr. G. Timmers for his expert help in performing the experiments.

9 References

ALONSO, E.E., GENS, A. and HIGHT, D.W. (1987), Special problem soils: general report. *Proceedings 9th European Conference on Soil Mechanics and Foundation Engineering*, Balkema, Rotterdam, vol.3, pp 1087-1146.

AMANULLAH, M., MARSDEN, J.R. and SHAW, H.F. (1994), Effect of rock-fluid interactions on the petrofabric and stress-strain behaviour of mudrock, *Eurock '94*, SPE/ISRM Rock Mechanics in Petroleum Engineering, A.A. Balkema, Rotterdam, pp. 85-92.

ARSLAN, A., SCHLANGEN, E, and VAN MIER, J.G.M. (1995), Effect of model fracture law and porosity on tensile softening of concrete. *Fracture Mechanics of Concrete Structures.* (ed F.H. Wittmann), AEDIFICATIO Publ., Freiburg, pp.45-54.

BEAR, J. and BACHMAT, Y. (1991), *Introduction to modeling of Transport Phenomena in Porous media.* Kluwer Academic Publishers, Dordrecht.

BIOT, M.A. (1941), General theory of three-dimensional consolidation. *J.Appl.Phys.* 12:155-164.

BIOT, M.A. (1973), Nonlinear and semilinear rheology of porous solids. *J.Geoph.Res.* 78(23): 4924-4937.

BOURDAROT, E., MAZARS, J. and SAOUMA, V. (1994), *Dam fracture and Damage.* A.A. Balkema, Rotterdam.

BRÜHWILER, E. and SAOUMA, V.E. (1990), *Fracture Mechanics of Concrete Gravity Dams: Effect of Hydrostatic Pressure on Fracture of Concrete. Vol 1. Test Report.* University of Colorado, Boulder (CO).

CLAUSS, G., LEHMANN, E. and OSTERGAARD, C. (1992), *Offshore Structures. Vol. 1: Conceptual Design and Hydromechanics.* Springer-Verlag, London.

DEFAY, R., PRIGOGINE, I. and BELLEMANS, A. (1966), *Surface Tension and Adsorption.* Longmans, Green & Co Ltd., London.

DESROCHES, J. and THIERCELIN, M. (1993), Modeling the propagation and closure of micro-hydraulic fractures. *IJRM* 30:1231-1234.

DULLIEN, F.A.L. (1992), *Porous Media: Fluid transport and Pore Structures.* Academic Press Inc., N.Y..

GOWD, N. and RUMMEL, F. (1980), Effect of confining pressure on the fracture behaviour of porous rocks. *Int. J.Rock Mech.Min.Sci.&Geomech.Abstr.* 17:225-229.

GREGG, S.J. and SING, K.S.W. (1982), Adsorption, *Surface Area and Porosity.* Academic Press, London.

HANDIN, J. and HAGER, R.V. Jr. (1957), Experimental deformation of sedimentary rocks under confining pressure: tests at room temperature on dry samples. *Am.Assoc.Petr. Geol.Bull.* 41:1-50.

HILLER, K.H. (1964), Strength reduction and length changes in porous glass caused by wtaer vapour adsorption, *J.Appl.Phys.* 35(5):1622-1628.

HILLERBORG, A., MODÉER, M. and PETERSSON, P.E. (1976), Analysis of crack formation and crack growth in concrete by means of fracture mechanics and finite elements. *Cement and Concrete Res.* 6(6):773-782.

HETTEMA, M. (1996), *The Thermo-Mechanical Behaviour of Sedimentary Rock: An Experimental Study.* EburonP&L, Delft.

HORDIJK, D.A., VAN MIER, J.G.M. and REINHARDT, H.W. (1989), Material Properties. *Fracture Mechanics of Concrete. From Theory to Application* (ed L.Elfgren), Chapman and Hall, London, pp 67-132.

HSU, T.T.C. (1963), Mathematical analysis of shrinkage stresses in a model of hardened concrete, J.Am. Concrete Inst. 2: 209-224.

INGRAFFEA, A.R., SHAFFER, R.J. and HEUZE, F.E., *FEFLAP: A Finite Element Program for Analysis of Fluid-driven Fracture Propagation in Jointed Rock.* Vol 1., Lawrence Livermore Laboratory, Report no. UCID-20368,

ISRAELASHVILI, J.N. (1985), *Intermolecular and Surface Forces with Application to Colloidal and Biological Systems.* Academic Press, London.

JAMET, P., MILLARD, A. and NAHAS, G. (1984), Triaxial behaviour of a micro-complete stress-strain curve for confining stresses ranging from 0 to 100 MPa, *RILEM-CEB Symposium on Concrete under Multiaxial Conditions.* INSA Toulouse, Vol.1, pp 133-140.

KUPFER, H. (1973), *Das Verhalten des Betons unter mehrachsiger Kurzzeitbelastung unter besonderer Berücksichtigung der zweiachsiger Beanspruchubg.* Deutscher Ausschuss für Stahlbeton, Vol. 269.

MILLS, R.H. (1960), Strength-maturity relationships for concrete which is allowed to dry. *Studies in Concreting in Hor Countries* (eds. R. Shalon and D. Ravina), pp. 1-28.

MINDESS, S. (1989), Interfaces in concrete. *Material Science of Concrete I.* (ed J. Skalny), Am.Concrete Soc., pp. 163-180.

MINDESS, S. and Young, J.F. (1981), *Concrete.* Prentice and Hall Inc.

NEVILLE, A.M. (1977), *Properties of Concrete.* Pitman Publ. Ltd., London.

NEWMAN, J.B. (1978), Concrete under complex stresses. *Developments in Concrete Technology - 1* (ed F.D. Lydon), Appl.Sci.Publ.Ltd., London, pp 151-220.

NILSON, R.H. (1981), Gas-driven fracture propagation. *J.Appl.Mech.* 48:757-762.

NORRISH, K. (1954), The swelling of montmorillonite. *Disc. Faraday Soc.* 18:120-134.

ONAISI, A., DURAND, C. and AUDIBERT, A. (1994), Role of hydration state of shales in borehole stability studies, *Eurock '94*, SPE/ISRM Rock Mechanics in Petroleum Engineering, A.A. Balkema, Rotterdam, pp. 275-284.

PETERSSON, P.-E. (1981), *Crack Growth and Development of Fracture Zones in Plain Concrete and Similar Materials.* Report TVBM-1006, Lund Inst. of Techn., Sweden.

POWERS, T.C. (1968), Mechanics of shrinkage and creep of hardened cement paste. The structure of concrete and its behaviour under load. *Proc. C&CA*, London.

REINHARDT, H.W. (1985), *Beton als Constructiemateriaal, Eigenschappen en Duurzaamheid.* Delft University Press, Delft.

ROSSI, P. and BOULAY, C. (1990), Influence of free water in concrete on the cracking process. *Mag. of Concrete Res.* 42(152):143-146.

SAOUMA, V.E., BROZ, J.J., BOGGS, H.L. and BRUHWILER, E. (1989), A comprehensive inverstigation of fracture mechanics of concrete dams. *ICOLD 57-th Executive Meeting on Analytical Evaluation of Dam Related Safety Problems*, pp 1-15.

SCHATZ, J.F. (1976), Models of inelastic volume deformation for porous geological materials. *The Effects of Voids on Material Deformation* (eds S.C. Cowin and M.M.Carroll), ASM, New York, pp 141-170.

SCHMITT, D.R. and ZOBACK, M.D. (1992), Diminished pore pressure in low-porosity crystalline rock under tensional failure: apparent strengthening by dilatance. *J.Geoph.Res.* 97(B1): 273-288.

SCOTT, T.E. and NIELSEN, K.C. (1991), The effect of porosity on the brittle-ductile transition in sandstones. *J.Geophys.Res.* 96:405-414.

SCRIVENER, K.L. (1989), The microstructure of concrete. *Material Science of Concrete I.* (ed J. Skalny), Am.Concrete Soc., pp. 127-161.

THIERCELIN, M.J., JEFFREY, R.G. and BEN-NACEUR, K. (1987), The influence on fracture toughness on the geometry of hydraulic fractures. SPE 16431, *SPE/DOE Low Permeability Reservoir Symposium*, Denver (CO).

TWORT, A.C., LAW, F.M. and CROWLEY, F.W. (1994), *Water Supply.* Arnold, London.

VAN MIER, J.G.M. (1991), Mode I fracturing of concrete: crack growth and crack interface grain bridging. *Cement and Concrete Res.* 21:1-15.

VAN MIER, J.G.M. (1992), Scaling in tensile and compressive fracture of concrete. *Application of Fracture Mechanics to Reinforced Concrete.* (ed. A. Carpenteri), Elsevier Applied Science, London/ New York, Chapt. 5.

VAN MIER, J.G.M. (1997), *Fracture Processes in Concrete.* CRC Press, Boca Raton (Fl).

VISSER, J.H.M. (1997), *Extensile Hydraulic Fracturing of Porous Materials.* Ph.D. Thesis Delft University of Technology (to appear).

VISSER, J.H.M. and VAN MIER, J.G.M. (1994), Deformation controlled hydraulic fracture experiments on concrete, *Dam fracture and Damage.* (eds. E. Bourdarot, J. Mazars and V. Saouma), A.A. Balkema, Rotterdam, pp 133-141.

WALSH, J.B. (1965), The effect of cracks on the compressibility of rock. *J.Geoph.Res.* 70(2): 381-411.

WITTMANN, F.H. (1977), Grundlagen eines Modells sur Beschreibung charakteristischer Eigenschaften des Betons. *Deutscher Ausschuss für Stahlbeton* 290:43-101.

YATES, D.J.C. (1954), The expansion of porous glass on the adsorption of non-polar gases. *Proc. Royal Soc. London*, A224:526-543.